A Novel Interpretation of Polarization Effects in Measured Nucleon Form Factors

Matt Enright

Submitted in partial fulfillment of the
requirements for graduation with Honors
from the South Carolina Honors College.

Spring 2008

Approved:

Dr. Ralf W. Gothe
Thesis Director
Department of Physics and Astronomy

Dr. Gary S. Blanpied
Second Reader
Department of Physics and Astronomy

Dr. Davis Baird
Dean, South Carolina Honors College

Contents

List of Figures

List of Tables

Thesis Summary

Beginning with the Democritic postulate of an atomic division of all matter, science has strove to dig ever deeper into what makes up the world we interact with every day. When the atom was discovered to be a composite particle, further probing the tiniest scales imaginable discovered the nucleus, and yet it too was later found to be made up of its own compound particles. These protons and neutrons, called baryons, or more specifically the nucleons, were eventually discovered to be part of an isospin doublet, impossibly composed of even more fundamental constituents, dubbed the quarks. The interaction of these quarks with one another manifested itself in the observable properties that distinguished the two nucleons and suddenly, the nucleons themselves were not unique configurations of these pointlike constituents, but merely two parts of a veritable menagerie of baryons. Neither was that the end of the possibilities arising from quark interactions another class of particles, called the mesons, were too the product of interactions between pairs of quarks. Yet for all of the discoveries made and attributed to the quarks over the last half-century, there is almost no concensus explanation that can encapsulate and predict their behavior within these composite particles. So-called intermediate energy physics attempts to measure their interactions through nuclear reactions, measuring decay products, energy levels, and other principal quantum numbers, in an ongoing effort to definitively describe the structure of these particles protons, neutrons, mesons, etc. (collectively, the hadrons). They are known to be 'excitable' that is, they can be induced over

short time-spans to new configurations, known as resonances, and they are known to decay through different channels, producing in turn new hadronic or leptonic products, that allow for distinguishing these resonances from ground-state, or relatively speaking stable configurations of the constituent quarks. One of the most powerful tools available to physicists in the study of these composite particles are the electromagnetic form-factors, functions that describe the 'shape' of the particle and it's resistance to decomposition in reactions.

There exist two tested experimental methods to extract the electromagnetic form-factors from the nucleons, a method known as Rosenbluth scattering that involves an elastic (non-destructive) reaction between electrons and the target nucleons. By measuring the recoil of the proton and the deflection of the electrons, the kinematics of the experiment allow for the calculation of the measured form-factors. A similar elastic reaction can also be done using polarized electrons in which the chief indicator of the target nucleon's form-factor is measured through the polarization of the recoiling nucleon, transferred to it by the electron. These methods are independently verified to measure these functions, yet have a surprising disparity when the normalized form-factor ratio (the standard metric of comparison is the ratio of the electric to the magnetic form-factor) is compared in each case. Whereas the Rosenbluth method exhibits a fairly constant unity relationship through the range of momentum transfer, in a polarization-transfer reaction this quantity falls off quickly as the magnitude of the momentum transfer increases. The incompatibility of these results is unexpected from and unexplained by the theoretical model, and the attempts to reconcile them take a phenomenological approach that introduces corrective processes and higher-order terms in the interaction potential that are fixed by parameters, not necessity and are often model-dependent.

In order to examine the fundamental differences in the processes and reactions at the root, one can instead appeal to the derivation of these form-factor extractions from

the experimental observations. By being careful to avoid making any assumptions to the equality and correlation of the form-factors measured through different processes, it is possible to independently define form-factors for each of the reactions in a slightly more cumbersome, but formally equivalent and indisputably valid, representation of the nucleon's shapes in terms of the experimentally detectable kinematics.

This representation of the separated form-factors actually can be shown to correspond directly with a particular set of nucleon states. These states, currently being explored at the University of Washington and elsewhere [15, 16], indicate that the nucleons may not have, as previously thought, a spherical shape in all circumstances. Certain configurations of the spin of the internal quarks can cause a deformation in the shape of the nucleon. This is a phenomenal result, but taken together with the form-factor extractions above can be directly extended to the problem of form-factor measurement. The polarization state of the recoiling nucleon is represented in a basis of two spin-directions - directions that correspond directly to two of the primary spin-states examined in the deformation work. This would seem to indicate that when the experiment is being carried out on a particle in one of these states, its shape (and thus, its form-factors) is significantly different than its shape in a state such as that measured by the Rosenbluth cross-section.

With this realization, it becomes trivial to explain the difference in the form-factors. As predicted by the deformations of the nucleon in the polarization-transfer reaction, the magnetic form-factor is either extended along its transverse or longitudinal axis, and when the ratio for this experiment is calculated by the same method as for the Rosenbluth reaction, the analagous quantity (a combination of the state-specific magnetic form-factor terms and the unaltered electric form-factor) falls off as momentum transfer increases, just as seen with the experimental results. The error then, in the current view of form-factor measurement, is not one of experimental deficiency or systematic inaccuracies as has been proposed, but it is simply an inap-

propriate interpretation of the results that arises from comparing two fundamentally different quantities - the spherical (Rosenbluth) form-factors, and the deformed and non-spherical ones.

This realization not only resolves the issue of incompatible results (by noting that they are not really incompatible at all, simply incomparable), but it indicates that the internal spin-state of the nucleon, considered indeterminate by quantum field theory in the situation where the composite particle is being probed, is accessible from currently feasible (and indeed common) experimental techniques, by measuring the independent separated form-factors and examining their correspondance to the deformation operators.

Abstract

A new method of interpretation is applied to the results of polarization-transfer through elastic electron-nucleon scattering that offers an explanation for the noted experimental inconsistencies of electromagnetic form-factor extraction with those of the classical Rosenbluth scattering techniques. New research on the position and momentum-space charge density and magnetic moments of the nucleons indicates that there may be non-spherical deformations in the nucleon shapes that result from the alignments of nucleon and constituent quark spins. The application of these results to Rosenbluth and polarization-transfer scattering cross-sections indicates that, while Rosenbluth scattering projects spherical form-factors, the polarization-transfer method is sensitive to these deformations and exhibits a prolate (and thus larger) magnetic charge distribution that lowers the form-factor ratio from what is observed in the spherical (Rosenbluth) case, in direct correspondance with the existing body of experimental data. This interpretation also allows for the possibility of directly measuring these deformations in the nucleon shapes, and consequently, directly the alignment of the constituent quark spins with respect to that of the nucleon, quantities previously thought inaccessible experimentally due to the Wigner-Eckhart theorem for spin-$\frac{1}{2}$ particles.

Chapter 1

Introduction

The 1918 discovery of the proton by Rutherford (and Chadwick's unearthing of it's isospin partner the neutron fourteen years later) ignited the world of subatomic physics; gone were the notions of a fundamental, elementary nucleus and the idea of a static atomic structure. Rapidly following were the discoveries of particles more fundamental than these nucleons and an entire pantheon of particles built up in a similar way from these newly observed constituent partons. The new picture of the proton and neutron was not one of indivisible charged balls but of strongly interacting and dynamic collections of confined quarks. With contributions from Murray-Gell Mann, Kazuhiko Nishijima, George Zweig and others, a model of 'strong' particles that fit into the SU(3) extension of the existing Pauli-Dirac mathematics for electroweak interactions was developed that gave predictive rise to the classes of hadrons observed in nature: 3-quark fermionic particles, or baryons, and 2-quark bosonic particles, called mesons.

With this new picture, however, the descriptions of these particles required a new understanding of their interactions, given in terms of these quarks and their unfamiliar means of combination. This is the heart of the field of quantum chromodynamics, the formalism of these particles, and it is one of the frontiers of modern physics. The

classification of hadronic matter and the elucidation of a sub-hadronic description of matter aims for the resolution of the missing resonance problem, the $\eta - \eta\prime$ inconsistency, a description of the decuplet (octet) baryon (meson) states and a host of other issues that are not well understood within the quark structures predicted by the Standard Model.

One way that these structures are analyzed is through form-factors, functions that describe the resiliency against decomposition of a particle with internal structure (see Chapter 2). The extraction of these form-factors for the proton and the neutron from elastic electron scattering is a crucial tool in the study of sub-nuclear structures, and the Sachs electric and magnetic form-factors of the nucleons are well-described in such a process by the Rosenbluth cross-section [18] (see section 2.2). These form-factors can be regarded as the 'shape' of the nucleon in the sense that a Fourier transformation links the electric form-factor to the charge-density distribution and the magnetic form-factor to the anomalous magnetization, or the density distribution of the magnetic moment, of the nucleon. In the formalism of quantum electrodynamics, this scattering process is thought to be well understoond by the mechanisms of virtual photon exchange, yet when applied to a polarization-transfer measurement (see section 2.3) there is a marked deviation from the form-factors exhibited in Rosenbluth scattering that grows with Q^2 [10]. This discrepancy is clearly the result of a mechanism beyond the experimental or systematic errors of the scattering processes, which have been probed and measured thoroughly at high momentum-transfers [11, 12, 9] in an attempt to explain the divergence of the form-factors as observed. This experimental result leads, at first blush, to one of two possible explanations: either the (previously assumed) interactions are not accurately describing the cross-section of the scattering processes, or the form-factors are not described by the cross-sections as previously thought.

The currently fashionable theoretical approach to resolving these issues involves

measuring the contributions of additional processes and higher-order interactions between the electron and the target nucleon that offer significant corrections to the Rosenbluth cross-section [5, 2]. These corrections are highly model-dependent, but in general they bring the form-factor ratios of the Rosenbluth process closer in line with the lower polarization-transfer measurements at higher momentum transfers. Current research is underway to measure these corrections by the analysis of assymetries between the cross-sections of electron-nucleon scattering and positron-nucleon scattering reactions with experiments proposed at Jefferson National Laboratory and at the Siberian VEPP-III storage ring facility [4], but there exists currently no definitive application of these corrections or a canonical theoretical motivation of their significance.

This thesis endeavors to motivate an alternate interpretation of the differences between form-factor observables in Rosenbluth scattering and in polarization-transfer measurements through first principles with minimal assumptions and without appealing to contrived externalities such as model-dependent side-effects or parameter-driven corrections. A discussion on the form-factors themselves and their properties and extractions, as well as a discussion of the experimental techniques for measuring them will be used to set the background for this approach in Chapter 2. Chapter 3 then will summarize the salient points of exciting new research being done by Drs. Gerald Miller (University of Washington) and Alexander Kvinikhidze (The Mathematical Institute of the Georgian Academy of Sciences) [15, 16] that indicates non-spherical properties of the nucleons under certain observational conditions. These observations and findings are calculated using a relativistic light-front frame, the mechanics of which can be found detailed in the back-matter (Appendix B). Using the background established in the first parts of this paper, Chapter 4 will attempt to bring the two fundamental ideas together and, using new data from polarization-transfer scattering experiments, illustrate the synthesis of the new interpretation of

form-factor results that points to an intuitive view of the nucleon and allows for the possibility of extracting further information previously thought unavailable to experimental observers, some of which will be discussed in the concluding remarks (Chapter 5) on significant possibilities that can be built on the simplified interpretation presented herein.

Chapter 2

Electromagnetic Form-Factors

Quantum mechanics predicts that a Dirac (point-like) particle of spin-$\frac{1}{2}$ will exhibit a magnetic moment with a g-factor of 2, but experimental observations in the early 20^{th} century showed a proton magnetic moment with $g = 5.586$. This provided the first clear evidence that the proton is not, in fact, a Dirac particle and thus that it has a definite substructure, particularly an electromagnetic one. The first explorations of this structure confirmed that descriptions of this structure, called form-factors, were dependent only on Q^2, or the square of the transferred four-momentum in the scattering process[7]. These form-factors, F_1 and F_2, are called the Dirac and Pauli form-factors, respectively, and they can be re-written to define form-factors which isolate the electric and the magnetic properties, as follows:

$$G_E = F_1 - \tau\kappa F_2 \tag{2.1a}$$

$$G_M = F_1 + \kappa F_2 \tag{2.1b}$$

These are the Sachs form factors, and they will be used (unless explicitly noted otherwise) for the remainder of this thesis in the discussion of form-factors. The subscripts E and M denote electric and magnetic components, respectively. τ is the kinematic parameter, equal to ${}^{Q^2}/_{4M}$ for a nucleon mass of M, and κ is the anomalous

magnetic moment of the nucleon[1], that is, the deviation of the magnetic moment from the ideal predicted for a Dirac particle [17]. The electric and magnetic Sachs form-factors may be extracted directly from experimental cross-sections; see the following sections 2.2 and 2.3 for more details on those calculations.

The Sachs form factors are important descriptions of the nucleon shapes not only because of their relevance to the elastic scattering cross-sections, but because they are also directly related to the electric charge distribution and the magnetization functions (for G_E and G_M respectively) via the Fourier transformation in the non-relativistic limit. This makes an accurate measurement of these form-factors paramount in studying the spin structure of the nucleon, in addition to the development of QCD formalism and various quark models of the nucleonic interactions and hadronic degrees of freedom.

Both the electric and the magnetic form factor follow the same general shape, that of a dipole (2.2),

$$G_D = \left[1 + \frac{Q^2}{0.71}\right]^{-2} \tag{2.2}$$

which the form factors are typically normalized to, with the magnetic form factor also typically shown normalized to the anomalous magnetic moment. The limit cases as $Q^2 \to 0$ for these functions have been both experimentally and theoretically shown to correspond directly to the nucleon charge (for G_E) and the magnetic moment (for G_M), respectively. The following sections 2.1 and 2.2 concern the formulation of these form-factors as coefficients to the scattering cross-section.

2.1 Elastic scattering

A coherent elastic scattering process is one in which the quantum numbers of the target/scattering particles are unmodified, and there is no internal energy added to

[1]Where κ is $\frac{\mu_p}{\mu_N} = 2.79$ for the proton, and $\frac{\mu_n}{\mu_N} = -1.91$ for the neutron. μ_N is the nuclear magneton.

the system, i.e. as in a resonance or excitation state. In the case of an electron scattering on a point-particle, the cross-section is calculated as follows using the Feynman diagram technique. Summing the interaction operators at the vertices (both

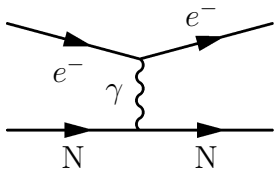

Figure 2.1: Feynman diagram of an electron scattering off of a point-particle N.

$\sqrt{\alpha}$, α the electromagnetic coupling constant), the scattering process represented (an electron with initial energy E being scattered at an angle of θ off of a point-like nucleon target of charge Ze), one obtains the Rutherford cross-section (2.3).

$$\frac{d\sigma}{d\Omega} = \frac{Z^2\alpha^2(\hbar c)^2}{4E^2\sin^4\frac{\theta}{2}} \tag{2.3}$$

This is correct in the relativistic limit up to incorporating spin-effects of the electron or the target, and neglecting the recoil effect on the target, i.e. the momenta of the incoming and outgoing electron are considered to be the same, and likewise with the target particle. This is adapted from the nuclear scattering technique used by Rutherford by replacing the nuclear form-factor $|F(\mathbf{q})|^2$ with a δ-function to approximate a structureless point-particle [17].

In order to incorporate the spin effects, relevant in relativistic conditions, an additional term is required to ensure conservation of helicity (in the limit $\beta \to 1$). This leads to the Mott cross-section (2.4), and it is correct in the relativistic limit for elastic scattering without recoil effects in the target [17].

$$\left(\frac{d\sigma}{d\Omega}\right)^*_{Mott} = \left(\frac{d\sigma}{d\Omega}\right)_{Rutherford}\left[1 - \beta\sin^2\frac{\theta}{2}\right] \tag{2.4}$$

Note that the Mott cross-section takes into account only the non-spin-flip reaction. If

the target particle has spin, total angular momentum can be conserved without the helicity of the electron necessarily being conserved, i.e. in the case of backscattering through 180 deg [17].

This cross-section gets closer to accurately describing the process of interest here by replacing a nucleus with a nucleon as the target particle and allowing the reaction to couple to a spin flip, but another major assumption needs to be removed from the formulation: that of no recoil to the target particle. The mass of the nucleon (approx. $940 MeV/c^2$) is of the same order of the typical electron energies required in an elastic scattering, so there is a scaling factor of the electron energies required to take into account the energy transfer (no longer negligible) to the nucleon. This also, since we are firmly in the relativistic case, requires use of the four-momentum transfer Q^2 rather than the three-momentum transfer $\mathbf{q}$ [17].

$$\left(\frac{d\sigma}{d\Omega}\right)_{Mott} = \left(\frac{d\sigma}{d\Omega}\right)^{*}_{Mott} \frac{E'}{E}\left[1 + 2\tau \tan^2\frac{\theta}{2}\right] \tag{2.5}$$

The additional term here arises from the interactions of the nucleon magnetic moment with the field of the electron current. This term exhibits the spin-flip component of the interaction, and becomes more apparent when expressed in terms of the Sachs form-factors later. τ is the kinematic parameter, equal to $\frac{Q^2}{4M^2}$, introduced to normalize the magnitude of the interaction to that of the electron deflection, obviously linear in Q^2. This quantity's appearance in the matrix element will come up in normalizing all of the magnetic interactions in the following extension of the cross-sections.

2.2 Rosenbluth method

As the first electron-nucleon scattering experiments began to take place, discrepancies were noted between the expected cross-section (modified Mott, (2.5) above), and that observed from the measurements. It was this result that led to the under-

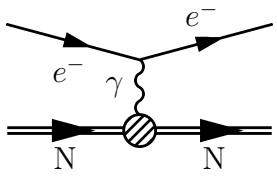

Figure 2.2: Feynman diagram of an electron scattering off of a compound nucleon target.

standing of the proton as a compound particle (Figure 2.2, and the modification of the Mott scattering cross-section to account for a spin-flip interaction with the nucleon. This modification results in the Rosenbluth equation (2.6) as a cross-section for the electron-nucleon scattering process [18].

$$\frac{d\sigma}{d\Omega} = \left(\frac{d\sigma}{d\Omega}\right)_{Mott} \left[\frac{G_E^2(Q^2) + \tau G_M^2}{1+\tau} + 2\tau G_M^2(Q^2)\tan^2\frac{\theta}{2}\right] \tag{2.6}$$

For brevity, the virtual photon polarization parameter $\epsilon = [1 + 2(1+\tau)\tan^2\frac{\theta}{2}]^{-1}$ is introduced.

$$\frac{d\sigma}{d\Omega} = \left(\frac{d\sigma}{d\Omega}\right)_{Mott} \frac{1}{1+\tau}\left[G_E^2(Q^2) + \frac{\tau}{\epsilon}G_M^2(Q^2)\right] \tag{2.7}$$

Equations (2.6) and (2.7) are the key to this method of determining nucleon form-factors. For reasons which will become apparent in Chapter 4, the independently resolved values for the Sachs form-factors here will be denoted G_E^R and G_M^R when referring to the Rosenbluth separation method. The Mott cross-section is fixed by the kinematics, as are τ and θ, while the form-factors are dependent only on Q^2, so the extraction is done experimentally by varying the beam energy E and the scattering angle of the outgoing electron θ while keeping Q^2 constant. The data set over this range of kinematic values is then normalized to the Mott cross-section given in equation 2.5, eliminating the kinematic terms and yielding a linear function that is trivially seperated to give G_E^R and G_M^R. Repeating this process over a range of values for Q^2 gives the dependence of the form-factors, both of which, as mentioned above, are approximated well by the dipole (2.2).

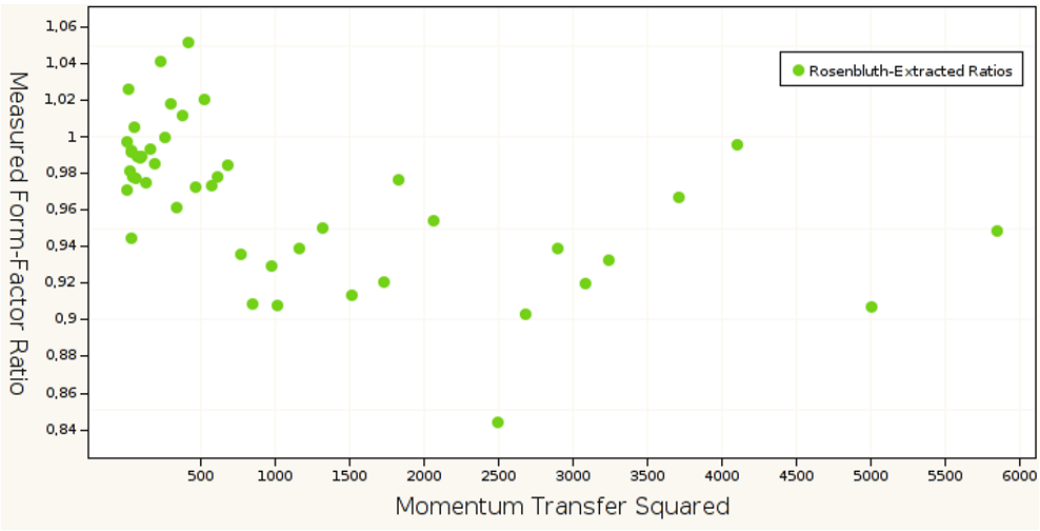

Figure 2.3: Normalized ratio of extracted form-factor values in the Rosenbluth process against Q^2 (in GeV^2).

Repeated execution of these experiments through a wide range of Q^2 values [8, 9] have shown that the ratio $\kappa G_E^R/G_M^R$ is relatively constant at unity in Q^2, as shown below in Fig. 2.2.

2.3 Polarization transfer method

Polarization transfer experiments are likewise elastic processes, done by scattering longitudinally polarized electrons off unpolarized protons (Fig. 2.3). The recoiling proton is measured and will subsequently exhibit polarization in both the transverse and longitudinal directions with respect to the momentum directon of the proton in the scattering plane (all of the out-of-plane components are zero) 'received' from the electron. As noted above, this method exhibits a systematic decrease of the normalized electric to magnetic form factor ratio with increasing momentum transfer Q^2.

The polarization components in the scattering plane are given by the following

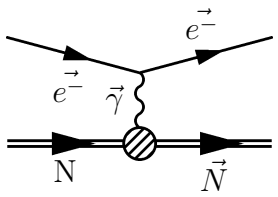

Figure 2.4: Feynman diagram of polarization transfer method of electron-nucleon scattering.

relations[1]:

$$I_0 P_t = -2\sqrt{\tau(1+\tau)} G_E G_M \tan\frac{\theta}{2} \tag{2.8a}$$

$$I_0 P_l = \frac{1}{M}(E+E')\sqrt{\tau(1+\tau)} G_M^2 \tan^2\frac{\theta}{2} \tag{2.8b}$$

I_0 is the averaged form-factor term in the Rosenbluth cross-section, $G_E^{R\,2} + \frac{\tau}{\epsilon} G_M^{R\,2}$. Equations 2.8 are trivially combined to get an expression for the ratio of form-factors (2.9), compared in Figure 2.3 with the same ratio as calculated from the cross-section in Rosenbluth scattering (Figure 2.2).

$$\frac{G_E}{G_M} = -\frac{P_t}{P_l}\frac{E+E'}{2M}\tan\frac{\theta}{2} \tag{2.9}$$

Obtaining this ratio experimentally is done differently than in Rosenbluth scattering, in that the form-factors are not independently observed[2], but measured as a ratio.

The polarization components of the recoiling nucleon target are measured with the use of, i.e, a focal plane polarimeter, simultaneously, as a function of the angular distribution of scattered particles in the polarimeter. The actual observable here is hA_cP_*, where h is the polarization of the electron beam, and A_c is the analysing power of the polarimeter [10]. In the ratio calculation then, of P_t/P_l, neither the beam polarization nor the polarimeter's analyzing power needs to be known in order to calculate the form factor ratio (2.9).

[2]This is to minimize systematic uncertainties and the requirements of experimental setups, not for any intrinsic prohibition of the measurement method. As noted in Chapter 4, measurements of

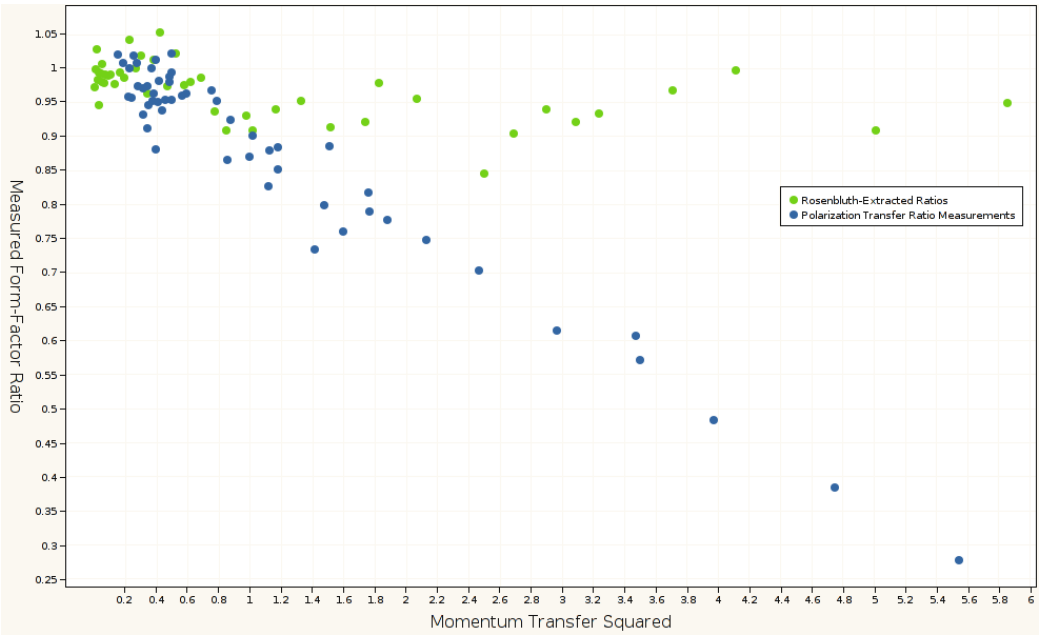

Figure 2.5: Plot of the experimentally observed ratios $\mu_N G_E/G_M$ against Q^2 (in GeV^2) for Rosenbluth and polarization transfer extractions.

2.4 Higher-order processes

The current research surrounding these two methods of nucleon form factor extraction has centered around the inclusion of additional processes, beyond the one-photon-exchange electromagnetic interaction assumed from the beginning in elastic scattering. While these higher-order or secondary interaction processes are typically negligible in their contribution to experimental cross-sections, there is hope that their effect on the Rosenbluth cross-section is significant enough to make up for the discrepancies in the high-Q^2 regime.

Studies of the higher-order two-photon exchange process have indicated that it is largely an angular-dependent contribution to the scattering cross-section, which makes it of particular interest in the Rosenbluth extraction in which the scattering angle is one of the key degrees of freedom for the form factor ratio at a given Q^2 measurement. These absolute corrections are not very strongly dependent on Q^2,

these quantities are rare, but by no means impossible, or even prohibitively difficult.

and so as the momentum transfer increases, the Rosenbluth cross-section is considerably reduced by the two-photon exchange process, as it is significant in extractions of the electric Sachs form factor, G_E. The process exhibits dependence on the virtual photon polarization parameter ϵ, roughly linear, in addition to the weakly increasing linear Q^2 dependence, which also supports the concept of a significant reduction in G_E for Rosenbluth separations (due to the decreasing dependence on G_E for the high-Q^2 cross-section). The polarization transfer measurements are not significantly adjusted by these higher-order corrections because the measurement of the polarization components and the cross-section are identically influenced by the process (both are sensitive only to the ratio G_E G_M as discussed above) and thus cancel [2].

The approaches here remain model-dependent and phenomenological at this point, but experimental techniques have been proposed to definitively measure the magnitude of contributions from two-photon exchange processes, most promisingly through comparison of the Rosenbluth cross-sections of $e^- p$ and $e^+ p$ scattering. The two-photon exchange amplitudes are charge-invariant for the scattering particle, where the wave function amplitudes are not, directly exhibiting an assymetry in the interference term of the interaction operator that should directly correspond to the two-photon amplitude [3].

An analysis of the global form factor data set has been performed [4] that applies a formal definition of the two-photon exchange operator [5] to existing cross-section data for Rosenbluth separation experiments at values of Q^2 up to 6 GeV^2. The extracted form factors from this data have been compared with the form factor ratios obtained from polarization transfer over a similar Q^2 range, where the results were found to more closely correspond, though with the aid of a model-adjustable parametrization that exhibited a significantly increasing error in the Rosenbluth values with Q^2.

Chapter 3

Nucleon Deformations

It is greatly material to the conclusions of the thesis to discuss current research on the deformed shapes of the nucleons, though an in-depth development of the theory is beyond this scope, and is left to the referenced works [15, 16, 14]. Qualitatively the result as detailed below indicates non-spherical shapes of the nucleons, dictated by the alignment between the spin of the proton and that of its constituent quarks, with well-defined deformations in the cases of (anti-)parallel and perpendicular spin axes. The formalism here is carried out in the light-front frame, the details of which are explored in Appendix B.

3.1 Spin-dependent density function

For a simple (proton-neutron) nuclear wave function with a central (radially symmetric) potential, the charge density $\rho(r)$ is the expectation of the density operator centered on the proton, $\delta(\mathbf{r} - \mathbf{r_p})$. If the proton is then constrained to have a spin in the direction of $\hat{\mathbf{n}}$, the density operator must be modified by that spin-projection, yielding the following charge density expression:

$$\rho(\mathbf{r}, \hat{\mathbf{n}}) = \left\langle \psi \left| \delta(\mathbf{r} - \mathbf{r_p}) \frac{1 + \sigma \cdot \hat{\mathbf{n}}}{2} \right| \psi \right\rangle \tag{3.1}$$

This technique has been used to witness deformations in the charge density of, i.e. the hydrogen atom for a spin-polarized nucleus. Applying similar techniques to the wave functions for an individual nucleon then, should make apparent any deformation present for particular angular momentum. Modifying (3.1) for the nucleon form-factor and the (relativistic) spin-projection in terms of the Dirac matrices, and introducing the quark charge operator $\hat{Q}$, the fully normalized calculation of the charge-density operator in momentum-space is as follows[15]:

$$\hat{\rho}(\mathbf{K}, \hat{\mathbf{n}}) = \frac{1}{(2\pi)^3} \int e^{\imath \mathbf{K}\cdot\mathbf{r}} \overline{\psi}(\mathbf{r}) \frac{\hat{Q}}{e} (\gamma^0 + \gamma \cdot \hat{\mathbf{n}} \gamma^5) \psi(\mathbf{0}) \mathrm{d}^3 x \tag{3.2}$$

The charge density is then just the expectation of that operator for a quark (in the nucleon described by ψ) with momentum $\mathbf{K}$ and spin in the direction $\hat{\mathbf{n}}$.

The fascinating result of this work is seen in the relativistic component of the Dirac spinors, where for $\| \mathbf{K} \| \ll m$, the charge density calculated is almost exactly spherical, but as $\| \mathbf{K} \|$ increases, nonspherical terms begin to dominate (see Figure 3.1); when the quark spin is parallel to the nucleon spin, the charge density exhibits a $\cos^2\theta$ form, leading to a prolate shape pinched around the center (imagine a peanut), and anti-parallel spin alignment is governed by $\sin^2\theta$, and appears toroidal. Further interesting configurations not of particular interest here come from i.e, perpendicular cases, which introduce an azimuthal angle ϕ dependence, and so on.

3.2 Form-factor extraction

Given the spin-dependent density function defined above, and given a spin-independent wave-function Ψ of the nucleon that includes the Dirac spinors of its constituent quarks and standard quantum number amplitudes, the form factors are (as classically) calculated from the nucleon interaction current $\mathbf{J}$. In the light-front formalism, the operator can be reduced to its longitudinal component, J^+, and the Pauli and

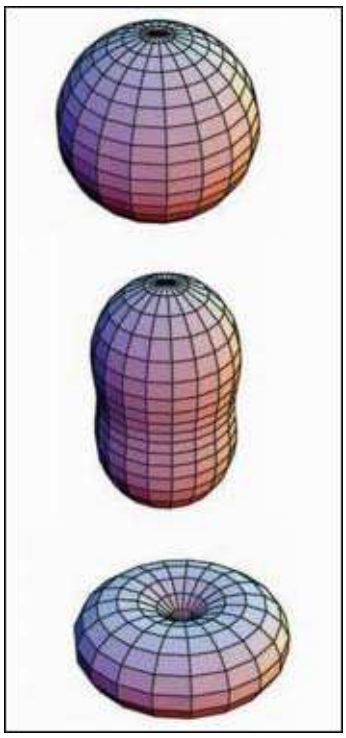

Figure 3.1: The nucleon shapes in the spherical (average) case, and those of the quark/nucleon spins parallel and anti-parallel.

Dirac form-factors are obtained as follows, isolating the spin-flip matrix element:

$$F_1(Q^2) = \frac{1}{P^+} \left\langle N,\uparrow \left| J^+ \right| N,\uparrow \right\rangle \tag{3.3a}$$

$$Q\kappa F_2(Q^2) = \frac{-2M_N}{2P^+} \left\langle N,\uparrow \left| J^+ \right| N,\downarrow \right\rangle \tag{3.3b}$$

The Sachs form factors are trivially calculated from these relations, using (2.1). The current operator needs to be defined to include the interaction and the transition matrix elements from initial to final states of the nucleon wave function. Since the calculation is fully relativistic and Ψ is a fermion (antisymmetric) wave function, the effect of the virtual photon's momentum transfer can be taken to act on a single quark, which, as will be seen below, dictates the spin of the nucleon. The antisymmetry ensures that a frame exists (the light-front frame, for one), where the total angular momentum contributed by the other two quarks cancels to zero, simplifying

the calculation[1].

This definition of the wave function and the current operator completely fixes the form factors by (3.3), and is dependent on the Dirac spinors of the constituent quarks, whose lower components contain the angular momentum terms that in turn affect the determination of the spin-dependent charge density function defined in section 3.1. This is a powerful tool that allows the interaction operator to determine both the shapes of the nucleon and the electromagnetic form factors, as further discussed in Chapter 4.

[1]Because of the quark's spinor structure, the magnitude of the spin is all that contributes: the nucleon helicity is not conserved by the transition as a whole (the F_1 matrix element does conserve helicity, that of F_2 does not)[6].

Chapter 4

Experimental Interpretation

Obviously, the results discussed previously are missing an important piece of understanding that links the two experimental methods and their contradictory measurements together in a unified phenomenological framework. Preliminary results from models of two-photon exchange contributions look to alleviate some of the difficulties in reconciling these two, but these calculations lack an *ab initio* justification for their impact, and they are highly dependent on data-tuned parameters to fit the experimental data. Even under the most successful of conditions, the corrections applied are unable to account for the entirety of the observed deviations at high Q^2 values. These are all signs of an effort to patch together an incorrect understanding of the underlying model, and appealing to the basics of the system indicates that there may be another way to interpret the results that can be directly and intuitively motivated.

Careful attention to the derivations in sections 2.2 and 2.3 may have raised concern over the careless use of the Sachs form-factors as defined for both experimental setups. The reason for this is historical, but the implicit assumption is made when separating the form-factors that they are equivalent under the circumstances of each experiment. Given the results concerning nucleon shapes introduced in Chapter 3,

and the discovery that non-spherical deformations are directly linked to the spins of the constituent quarks, it seems reasonable to attempt to construct a model that does not rely on the assumption that the electric and magnetic distributions of the nucleon are unaffected by these properties as well.

Returning to the interaction of the polarization transfer measurements, restricting the events of interest to elastic scattering events, both angular momentum and parity must be conserved. This limits the interaction to one mediated by a virtual photon of even parity that also couples to the spin-1/2 ground state of the nucleon. This disallows the electric dipole (E_1) contribution, which has negative parity, and the electric quadrupole (E_2) contribution, which has angular momentum $l = 2$ and thus couples only to the spin-$\frac{3}{2}$ or spin-$\frac{5}{2}$ final state baryon. The Coulomb monopole transition (C_0) has even parity, and no angular momentum contribution, so can couple to the nucleon with no spin flip, while the magnetic dipole (M_1) has even parity and an angular momentum of 1, corresponding to a spin-flip in the final state, so these are the interactions allowed by the scattering process.

Taking the relationship for polarization observables in PT-measurements from (2.8), they are now written below in such a way that no longer assumes that the form-factors are equivalent. Used is the convention introduced in the discussion of Rosenbluth scattering of superscripting the form-factor with an indicator of which case the function is applicable to; ^{R},^{l} or, ^{t} for the Rosenbluth (unpolarized), longitudinally polarized, or transversely polarized cases, respectively.

$$I_0 P_t = -2\sqrt{\tau(1+\tau)} G_E^t G_M^t \tan\frac{\theta}{2} \tag{4.1a}$$

$$I_0 P_l = \frac{1}{M}(E+E')\sqrt{\tau(1+\tau)} {G_M^l}^2 \tan^2\frac{\theta}{2} \tag{4.1b}$$

The I_0 definition does not need to be modified; as it is the average measurement of the nucleon shape as scaled by the cross-section and not subject to the particular

deformations in the polarization-transfer cases. This average of all nucleon shapes is simply spherical, which is the case exhibited by the Rosenbluth measurement, which then defines I_0 for a given Q^2.

$$I_0 = G_E^{R\,2} + \frac{\tau}{\epsilon} G_M^{R\,2} \tag{4.2}$$

Following the same derivation process as done in section 2.3, but taking care to keep the form-factors independent from one another, the following relationship is obtained:

$$\frac{G_E^t G_M^t}{G_M^{l\,2}} = \frac{-P_t}{P_l} \frac{(E+E')}{2M} \tan\frac{\theta}{2} \tag{4.3}$$

This quantity is exactly equivalent to what was previously assumed to be G_E/G_M (2.9). The plot shown in Figure 2.3 is, in this derivation, interesting for the sake of comparison, but should not be seen as an indictment of the experimental methods used: the datasets plotted are of different observable quantities which would not be expected from the model to be equal.

Further refining the separation of the form factors according to the theory of spin-dependent deformations, several other relationships can be gleaned from the model. The sensitivity of the polarization-transfer measurements to the spin of the internal quarks is predicated on the concept of alignment, enforced on the quark (and the proton as a whole) by the polarization of the virtual photon. The Wigner-Eckhart theorem prohibits measurement of a quadrupole magnetic moment contributions from the quarks: this still holds, but because of the spin-flip interaction operator for the M_1 multipole transition, the proton is forced to be spin-aligned along the axis of momentum transfer. Note as well, however, that this glimpse of knowledge is only possible for the M_1 photon exchange. In the other allowed process, the C_0 transition, there is no spin-flip (and no polarization-transfer). Since it is the spin-flip (an inherently magnetic transition) that allows knowledge of the alignment, there is no deformation

$\mathbf{Q}^2$	$\mathbf{P}_t$	$\mathbf{P}_l$	$\mathbf{G}_M^t$	$\mathbf{G}_M^l$	$\mathbf{G}_M^R$
0.8 GeV^2	-0.259	0.398	0.8900	1.4218	1.021
1.3 GeV^2	-0.214	0.437	0.8537	1.6114	1.057

Table 4.1: Separated form factor values from experimental data.

effect observed in the electric form factor, regardless of internal alignment.

This meshes with the understanding of the deformations as outlined in Chapter 3 as dependent on the angular momentum contributions of the nucleon wave-function. Existing experimental data to support or verify such an interpretation is difficult to come by, in no small part due to the method for most polarization transfer experiments discussed in Section 2.3, because by its nature the form factors are typically not measured independently. This poses a difficulty for the calculation of separated magnetic form-factors independently as in Appendix A and (4.1), which do require independent measurements of the in-plane polarization components P_t and P_l. The observables measured in many polarization transfer experiments are $P_t A_c h$ and $P_l A_c h$, where A_c is the analyzing power of the polarimeter and h is the helicity of the electron beam. Since these are measured independently, and in order to extract the form factor ratio only the ratio of the polarization components must be measured [10], the form-factor extraction is independent of the electron beam helicity and the polarimeter analyzing power [19]. With this knowledge, each of the polarization components can be known explicitly, and using (4.1) the independent form factors in both the transverse and longitudinal alignment cases can be found. Preliminary data points with all of the required information have been obtained from the E03-104 experimental run at Jefferson Laboratory [19] for two Q^2 values, as shown in Table 4 with the calculated form factor values below. The data for G_M^R is taken at the equivalent Q^2 from a global experimental data set [4].

Calculating the ratio from (4.3), the points lie on the same curve as the canonical G_E/G_M calculated from polarization transfer, which serves as a good check of the

interpretation's mathematical consistency. Also, as expected qualitatively from the nucleon deformation results in momentum space, [15], in the transverse polarization case, the magnetization density is contracted (see Figure 3.1, center), while for the longitudinal component it is extended (Figure 3.1, bottom), their values bracketing the spherical average calculated from Rosenbluth separation (Figure 3.1, top).

Chapter 5

Conclusions

Looking forward, the resulting intepretation presented here opens up significant opportunities for future understandings of the quark model and experimental probes of the structure of the nucleon. The interpretation offers an explanation for the observed discrepancies of the form factor ratios obtained from Rosenbluth separation and from polarization transfer measurements by removing the assumption that they be equivalent, neatly supported by current research on how the electric charge and magnetization densities (and by extension, the Sachs electric and magnetic form factors) are measured.

The preceding development of a form factor theory is carried out from basic principles without requiring any assumptions or a model-dependent ansatz to explain its qualitative interpretations. Future research along these lines is naturally drawn to either of two paths: further analysis of a broader experimental data set for polarization transfer scattering, subject to the availability of the independently measured polarization components as discussed above, and (currently investigated) attempts to extract a predicted function for the form factors (and the equivalent ratios) from the theory of spin-dependent nucleon deformations that can be experimentally verified with current and future measurements.

This also presents an opportunity for further understanding the spin structure of the nucleons by allowing (through measurement of the ratio in Eq. 4.3) experimental observation of the spin axis of the constituent quarks in elastic scattering without violating or requiring a spectroscopic quadrupole moment of the nucleon. The sensitivity of the polarization transfer measurements to the internal quark spins allows measurements to be taken that can exhibit these deformations, providing a possible experimental verification for the spin-dependent theory detailed in Chapter 3.

Appendix A

Separation of magnetic form factors

Let the cross section average I_0 be strictly determined (at a given value of Q^2) by the Rosenbluth interaction, since it is the average.

$$I_0 = G_E^R(Q^2)^+ \frac{\tau}{\epsilon} G_M^R(Q^2)^2$$

Using (2.8), specified as in (4.1), we can specify the polarization components (if measured independently) in terms of the relevant form factors. As before, the ^{R} superscript is dropped from the electric form factor, as G_E is unaffected by the deformations and is not sensitive to the spin-flip interaction.

$$P_t = \frac{-2\sqrt{\tau(1+\tau)} G_E G_M^t \tan\frac{\theta}{2}}{G_E^R(Q^2)^+ \frac{\tau}{\epsilon} G_M^R(Q^2)^2}$$

$$P_t = \frac{-2\sqrt{\tau(1+\tau)} G_E G_M^t \tan\frac{\theta}{2}}{{G_M^R}^2 \left(\left(\frac{G_E}{G_M^R} \right)^2 + \frac{\tau}{\epsilon} \right)}$$

$$P_t = \frac{G_M^t}{G_M^R} \frac{G_E}{G_M^R} \frac{-2\sqrt{\tau(1+\tau)} \tan\frac{\theta}{2}}{\left(\frac{G_E}{G_M^R} \right)^2 + \frac{\tau}{\epsilon}}$$

And similarly for the longitudinal recoil polarization component:

$$P_l = \frac{(E+E')\sqrt{\tau(1+\tau)}{G_M^l}^2 \tan^2\frac{\theta}{2}}{M\left(G_E^2 + \frac{\tau}{\epsilon}{G_M^R}^2\right)}$$

$$P_l = \left(\frac{G_M^l}{G_M^R}\right)^2 \frac{(E+E')\sqrt{\tau(1+\tau)}\tan^2\frac{\theta}{2}}{M\left(\frac{G_E}{G_M^R}\right)^2 + \frac{\tau}{\epsilon}}$$

With the exception of being scaled by a ratio of the relevant magnetic form factor to the average, both of these relations are dependent only on the ratio of electric to magnetic form factors obtained in the Rosenbluth (average) case. The ratio-dependent part of the equation is identical to that found in the canonical polarization transfer calculations, and so we trivially obtain the analagous ratio by dividing the polarization components as follows.

$$\frac{P_t}{P_l} = \frac{G_M^t}{G_M^R}\left(\frac{G_M^R}{G_M^t}\right)\frac{G_E}{G_M^R}\frac{-2M}{(E+E')\tan^2\frac{\theta}{2}}$$

$$\frac{P_t}{P_l} = \frac{G_E G_M^t}{{G_M^l}^2}\frac{-2M}{(E+E')\tan^2\frac{\theta}{2}}$$

This leads to the form factor ratio cited in (4.3), which is the same observable in polarization-transfer reactions that is canonically called "G_E/G_M" but is clearly seen here to differ from the spherical average exhibited in Rosenbluth scattering (G_E/G_M^R in the notation of this thesis).

$$\frac{G_E G_M^t}{{G_M^l}^2} = \frac{-P_t}{P_l}\frac{E+E'}{2M}\tan\frac{\theta}{2}$$

Appendix B

Light-front formalism

This is intended only as a quick reference for the conventions of the light-front formalism, sufficient for its brief use in describing the spin-dependent nucleon density operator (3.2) and the nucleon currents and wave-functions (3.3).

The light-front vector is defined as follows,

$$v \equiv \begin{pmatrix} v^+ \\ v^1 \\ v^2 \\ v^- \end{pmatrix}$$

where $v^\pm \equiv v^0 \pm v^3$, where v^i are the standard four-vector components. Also defined for convenience is $\mathbf{p}_\perp = (v^1, v^2)$, the perpendicular component of the vector [13].

The Dirac spinors can also be written in this coordinate-system, and are crucial to the development of the nucleon wave functions referred to in Chapter 3 [15]. Defined in the infinite-momentum frame, the spinors for a spin-1/2 particle with momentum $\mathbf{p}$ are as follows:

$$u(\mathbf{p}, \sigma) = \frac{\not{p} + m}{\sqrt{2m(m + p^0)}} u(\mathbf{0}, \sigma)$$

$$u(0, \uparrow) = (1, 0, 0, 0)$$

$$u(0,\downarrow) = (0,1,1,1)$$

Following the conventions of the light-front coordinates, these translate to the following expressions for spinors (only the spin-1/2 cases of up and down are relevant to this work, so are mentioned here):

$$u^{LC}(\mathbf{p},\uparrow) = \frac{1}{2\sqrt{mp^+}} \begin{pmatrix} p^+ + m \\ p^1 + \imath p^2 \\ p^+ - m \\ p^1 + \imath p^2 \end{pmatrix}$$

$$u^{LC}(\mathbf{p},\downarrow) = \frac{1}{2\sqrt{mp^+}} \begin{pmatrix} -p^1 + \imath p^2 \\ p^+ + m \\ p^1 - \imath p^2 \\ -p^1 + m \end{pmatrix}$$

For further information on these derivations and the relationship between light-front and infinite-momentum frame coordinates, or their application to the description of the nucleon wave functions, consult the references [13, 20, 15, 16, 14].

Bibliography

[1] A. I. Akhiezer and Mikhail. P. Rekalo. Polarization phenomena in electron scattering by protons in the high energy region. *Sov. Phys. Dokl.*, 13:572, 1968.

[2] J. Arrington. Evidence for two-photon exchange contributions in electron-proton and positron-proton elastic scattering. *Phys. Rev. C*, 69(3):032201, Mar 2004.

[3] J. Arrington. Implications of the discrepancy between proton form factor measurements. *Phys. Rev. C*, 69(2):022201, Feb 2004.

[4] J. Arrington, W. Melnitchouk, and J. A. Tjon. Global analysis of proton elastic form factor data with two-photon exchange corrections. *Phys. Rev. C*, 76(3), Sept 2007.

[5] P. G. Blunden, W. Melnitchouk, and J. A. Tjon. Two-photon exchange and elastic electron-proton scattering. *Phys. Rev. Lett.*, 91(14):142304, Oct 2003.

[6] V.M. Braun, A. Lenz, and M. Wittman. Nucleon form factors in qcd. *Phys. Rev. D*, 73(9), May 2007.

[7] E. E. Chambers and R. Hofstadter. Structure of the proton. *Phys. Rev.*, 103(5):1454–1463, Sep 1956.

[8] I. Qattan et al. Precision rosenbluth measurement of the proton elastic form factors. *Phys. Rev. Lett.*, 94(14), April 2005.

[9] M.E. Christy et al. Measurements of electron-proton elastic cross sections for $0.4 < q^2 < 5.5(gev/c)2$. *Phys. Rev. C*, 70(1):015206, Jul 2004.

[10] M.K. Jones et al. g_{E_p}/g_{M_p} ratio by polarization transfer in $\vec{e}p \to e\vec{p}$. *Phys. Rev. Lett.*, 84(7):1398–1402, February 2000.

[11] O. Gayou et al. Measurements of the elastic electromagnetic form factor ratio $\mu pgep/gmp$ via polarization transfer. *Phys. Rev. C*, 64(3):038202, Aug 2001.

[12] O. Gayou et al. Measurement of gep/gmp in $e \to p \to ep \to$ to $q2 = 5.6gev2$. *Phys. Rev. Lett.*, 88(9):092301, Feb 2002.

[13] M. Koster. Die berechnung der elektromagnetischen formfaktoren des nukleons sowie der n $\to \delta(1232)$ - übergangsformfaktoren mit hilfe des lichtkegelformalismus. Master's thesis, Universität Bonn, Physikalisches Institut, Jan 1996.

[14] G. A. Miller. Charge densities of the neutron and proton. *Phys. Rev. Lett.*, 99(11), Sept. 2007.

[15] Gerald A. Miller. Shapes of the proton. *Phys. Rev. C*, 68(2), August 2003.

[16] Gerald A. Miller and Alexander Kvinikhidze. Shapes of the nucleon. *Phys Rev. C*, 73(06523), Jun 2006.

[17] B. Povh, K. Rith, C. Scholz, and F. Zetsche. *Particles and Nuclei: An Introduction to Physical Concepts*. Springer-Verlag, Heidelberg, 4 edition, 1995, 2004.

[18] M.N. Rosenbluth. High energy elastic scattering of electrons on protons. *Physical Review*, 79(4):615–619, Aug 1950.

[19] S. Strauch. Private conversations, 2008.

[20] G. Wagner. Vergleich zweier relativistischer konstituentenquarkmodelle für baryonen. Master's thesis, Universität Bonn, Physikalisches Institut, Jan 1996.